PHYSICAL REVIEW B **72**, 214420 (2005)

Quantum spherical spin model on the AB_2 chain

M. H. Oliveira,* M. D. Coutinho-Filho,† and E. P. Raposo‡
Laboratório de Física Teórica e Computacional, Departamento de Física, Universidade Federal de Pernambuco, 50670-901, Recife, PE, Brazil

(Received 5 August 2005; revised manuscript received 21 October 2005; published 12 December 2005)

A quantum spherical spin model with an antiferromagnetic coupling J on the AB_2 chain is studied, whose topology is of interest in the context of ferrimagnetic polymers and oxocuprates. A ferrimagnetic long-range order is found at the only critical point $g=T=h=0$, where T denotes the temperature, h the magnetic field, and g the quantum coupling constant in energy units. The approach to the critical point, with diverging correlation length ξ and cell susceptibility χ_{cell}, is characterized through several paths in the $\{g,T,h\}$ parameter space: for $(T/J)\rightarrow 0$ and $g=h=0$, $\chi_{\text{cell}}\sim 1/T^2$, as also found in several classical and quantum spherical and Heisenberg models; for $(h/J)\rightarrow 0$ and $g=T=0$, $\chi_{\text{cell}}\sim 1/h$; and for $(g/J)\rightarrow 0$ and $T=h=0$, $\ln \chi_{\text{cell}}\sim 1/\sqrt{g}$, thus evidencing an essential singularity due to quantum fluctuations. In any path chosen the relation $\chi_{\text{cell}}\sim \xi^2$ is satisfied. For finite g and T a field-induced short-range ferrimagnetism occurs to some extent in the $\{g,T,h\}$ space, as confirmed by the analysis of the local spin averages, cell magnetization with a rapid increase for very low fields, and spin-spin correlation functions. The asymptotic limits of the correlation functions are also provided with respect to g, T, h, and spin distance. The analysis of the entropy and specific heat reveals that the quantum fluctuations fix the well-known drawback of classical spherical models concerning the third law of thermodynamics.

DOI: 10.1103/PhysRevB.72.214420 PACS number(s): 75.10.Jm, 75.50.Gg, 05.30.−d

I. INTRODUCTION

Since Stanley's pioneering work,[1] spherical models have attracted interest beyond Berlin and Kac's original proposal:[2] the spherical model as an alternative to the Ising model. Stanley discovered that the spherical condition maps onto the limit of infinite spin dimensionality of the Heisenberg classical model. As d-dimensional classical spherical models are exactly solved, these models have been largely used to explore the statistical mechanics of several systems, such as antiferromagnets,[3] including competing interactions[4] and Lifshitz points,[5] critical phenomena, including systems with long-range interactions,[6,7] topological considerations,[8] spin-charge effects in the context of the Hubbard model,[9] and disordered systems,[10] including spin glasses[11] and random field models.[12]

The original spherical model has a nonphysical behavior at zero temperature, i.e., its entropy and specific heat do not go to zero in this limit. This failure is corrected if one introduces a quantum character in this model. As a consequence, quantum versions of the spherical model have been applied to study spin glasses,[13] thermodynamic properties,[14] and quantum phase transitions in d-dimensional hypercubic lattices,[15] including random field effects[16] and ferromagnetic coupling with transverse field.[17]

In this work we are particularly interested in the thermodynamic and ground-state properties of the quantum spherical model on the AB_2 chain (see Fig. 1), whose experimental motivations[18] include inorganic ferrimagnetic polymer compounds, in which sites $A(B)$ may constitute a metal (ligand) atom (see Silvestre and Hoffman in Ref. 18 for a number of possible realizations) and oxocuprate compounds, such as $Ca_3Cu_3(PO_4)_4$, where $A(B)$ sites represent Cu atoms in a Cooper trimeric chain (see Drillon *et al.* in Ref. 18). Despite all the recent efforts through the study of the AB_2 chain in the context of models such as Hubbard and t-J,[20] quantum Heisenberg,[21] classical Heisenberg and Ising,[22] the influence of quantum fluctuations, as compared to thermal and magnetic field effects has not yet been fully comprehended in its thermodynamical and ground-state properties. Here we choose a first quantization scheme due to Obermair[19] to approach a quantum version of the spherical model in this topology, with a tunable parameter g to control the importance of quantum fluctuations in the system.

This paper is organized as follows. In Sec. II we introduce the model Hamiltonian on the AB_2 topology and diagonalize it to obtain the eigenmodes. The spherical condition is then derived from quantum thermal single- and two-operator averages. Section III is devoted to the calculation and analysis of several limits of local spin averages and cell magnetization and susceptibility, with respect to thermal and quantum fluctuations and the presence of magnetic field. Several spin-spin correlation functions are studied in detail in Sec. IV and the entropy and specific heat are considered in Sec. V. Although it is well known that spherical models embody ingredients not actually present in real materials, we believe that comparing our exact analytical results on these observables with experiments will lead to a gain in the understanding of quantum fluctuations close to the ground state of AB_2 spin systems. Finally, conclusions are presented in Sec. VI.

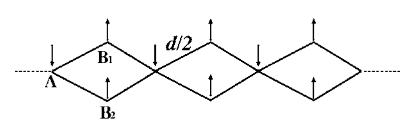

FIG. 1. Geometric model of the AB_2 chain displaying the ferrimagnetic long-range spin ordering for $g=T=h=0$. $d/2$ denotes the distance between A and B sites.

II. QUANTUM SPHERICAL SPIN MODEL AND THERMODYNAMICS

We assume that the spin $S=1/2$ degrees of freedom ($S_{i\alpha}$) are restricted to a certain axis (z axis), as in the classical spherical model.[2] We focus our attention on the effects of the interplay between quantum and thermal fluctuations on several properties of the system under an external magnetic field, such as local spin averages, cell magnetization and susceptibility, correlation functions, entropy, and specific heat.

The quantum counterpart of the spherical model implies in the quantization of the classical continuous spin variables in the form of spin operators $S_{i\alpha}$, whose average values may vary continuously with no upper and lower bounds, and quantum and thermal fluctuations subject to the mean spherical constraint

$$\sum_{i\alpha} \langle S_{i\alpha}^2 \rangle = \frac{N}{4}, \tag{1}$$

where latin letters index unit cells and greek letters index sites A, B_1, or B_2 (see Fig. 1); N is the total number of sites and $\langle \cdots \rangle$ indicates quantum thermal averages (see below). We introduce quantum fluctuations by assigning a canonical conjugate momentum $P_{i\alpha}$ to each spin degree of freedom, so that the following commutation relations hold ($\hbar=1$):

$$[S_{i\alpha}, S_{j\beta}] = 0, \quad [P_{i\alpha}, P_{j\beta}] = 0, \quad [S_{l\alpha}, P_{j\beta}] = i\delta_{lj}\delta_{\alpha\beta}, \tag{2}$$

where δ_{ab} denotes the Kronecker delta. The above features make the spin fields in quantum spherical models much more like unit quantum rotors[24] than standard quantum-mechanical spin operators usually considered in Heisenberg models.

We assume a first-neighbor antiferromagnetic (AF) interaction $J>0$ between spins at sites A and sites $B_{1,2}$.[23] In this way we have the following quantum Hamiltonian:

$$H = \frac{g}{2}\sum_{i\alpha} P_{i\alpha}^2 + \frac{J}{2}\sum_{\langle i\alpha, j\beta\rangle} S_{i\alpha}S_{j\beta} + \mu\sum_{i\alpha}\left(S_{i\alpha}^2 - \frac{1}{4}\right) - h\sum_{i\alpha} S_{i\alpha}, \tag{3}$$

where μ is the chemical potential, h is the magnetic field in energy units, $h \equiv \mu_{eff}H$, μ_{eff} is the effective Bohr magneton, and $k_B=1$ is the Boltzmann constant. In order to get a spin dynamics, the kinetic square term in $P_{i\alpha}$ is introduced in Eq. (3). This choice is not unique and is in fact determinant of the underlying spin dynamical behavior; however, it is by far the most usual one, as can be inferred from Refs. 13–17. In relation to this term, the tunable quantum parameter g, in energy units, controls the importance of the quantum fluctuations responsible for such spin dynamics. Further, one might also identify g with the inverse quantum coupling of the quantum $O(n)$ nonlinear σ model in the limit $n \to \infty$, whose $O(3)$ realization shares the same effective infrared behavior as the quantum antiferromagnetic Heisenberg model.

In order to diagonalize the Hamiltonian (3), we first introduce the set of boson operators $\{a_{i\alpha}^\dagger, a_{i\alpha}\}$ through the following transformations:

$$S_{i\alpha} = \frac{1}{\sqrt{2}}\left(\frac{g}{2\mu}\right)^{1/4}(a_{i\alpha} + a_{i\alpha}^\dagger), \tag{4}$$

$$P_{i\alpha} = \frac{-i}{\sqrt{2}}\left(\frac{2\mu}{g}\right)^{1/4}(a_{i\alpha} - a_{i\alpha}^\dagger), \tag{5}$$

which applied to Eq. (3) give rise to

$$H = \sqrt{2g\mu}\sum_{i\alpha}\left(a_{i\alpha}^\dagger a_{i\alpha} + \frac{1}{2}\right) - \frac{h}{\sqrt{2}}\left(\frac{g}{2\mu}\right)^{1/4}\sum_{i\alpha}(a_{i\alpha} + a_{i\alpha}^\dagger) - \mu\frac{N}{4} + \frac{J}{4}\sqrt{\frac{g}{2\mu}}\sum_{\langle i\alpha, j\beta\rangle}(a_{i\alpha}^\dagger a_{j\beta} + a_{j\beta}^\dagger a_{i\alpha} + a_{i\alpha}a_{j\beta} + a_{i\alpha}^\dagger a_{j\beta}^\dagger). \tag{6}$$

The symmetry between sites B_1 and B_2 is made evident through the definitions

$$a_{iB}^{(b)} = \frac{1}{\sqrt{2}}(a_{iB_1} + a_{iB_2}), \quad a_{iB}^{(a)} = \frac{1}{\sqrt{2}}(a_{iB_1} - a_{iB_2}), \tag{7}$$

where (b) indicates a bonding state and (a) an antibonding one. By Fourier transforming,

$$a_{i\alpha} = \sqrt{3/N}\sum_k e^{ikx_i}a_{k\alpha}, \quad k = \frac{2\pi}{N/3}v, \quad v = 0, \ldots, N/3 - 1, \tag{8}$$

along with the intracell translation transformation:

$$\psi_k = \frac{1}{\sqrt{2}}(a_{kA} + e^{-ik/2}a_{kB}^{(b)}), \quad \phi_k = \frac{1}{\sqrt{2}}(a_{kA} - e^{-ik/2}a_{kB}^{(b)}), \tag{9}$$

we define field operators associated with the global momentum conservation as follows:

$$\Delta_{k+} = \frac{1}{\sqrt{2}}(\psi_k + \psi_{-k}), \quad \Delta_{k-} = \frac{1}{\sqrt{2}}(\psi_k - \psi_{-k}), \quad k \neq 0; \tag{10}$$

$$\Theta_{k+} = \frac{1}{\sqrt{2}}(\phi_k + \phi_{-k}), \quad \Theta_{k-} = \frac{1}{\sqrt{2}}(\phi_k - \phi_{-k}), \quad k \neq 0; \tag{11}$$

$$\psi_0 = \psi_{k=0}, \quad \phi_0 = \phi_{k=0}. \tag{12}$$

In Eq. (9) the phase factor $e^{-ik/2}$ is due to the distance $d/2$ between sites A and $B_{1,2}$, where $d \equiv 1$ is the length of a unit cell (see Fig. 1). Moreover, one should notice that Eq. (9) involves only bonding operators. The reason for that lies in the fact that the transformation (7) already makes the Hamiltonian diagonal in the antibonding fields, such that, to pursue the diagonalization procedure, one no longer needs to consider these operators in the definition of new auxiliary fields from Eq. (9) on. We now use Bogoliubov transformations to diagonalize the resulting Hamiltonian in the $\{\Delta_{k+}, \Delta_{k-}, \Theta_{k+}, \Theta_{k-}, \psi_0, \phi_0\}$ space:

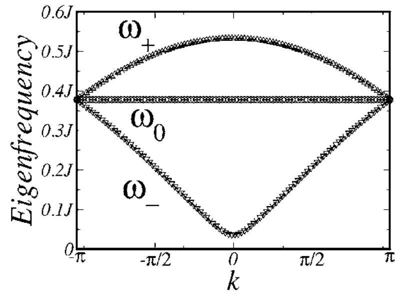

FIG. 2. Quantum eigenfrequencies $\omega_{k,m}$ as function of momentum k (in units of $1/d$) for $g=0.05J$, $T=0.05J$, and $h=0.05J$.

$$H=\sum_k \sum_{m=0,\pm1}\left[\omega_{k,m}\left(\lambda^\dagger_{k,m}\lambda_{k,m}+\frac{1}{2}\right)\right] - \frac{N}{3}\left(\frac{h^2(1+\sqrt{2}/2)^2}{4(\mu+\sqrt{2}J)}+\frac{h^2(1-\sqrt{2}/2)^2}{4(\mu-\sqrt{2}J)}\right)-\mu\frac{N}{4}, \quad (13)$$

where $\lambda_{k>0,1}=\alpha_{k+}$, $\lambda_{k<0,1}=\alpha_{k-}$, $\lambda_{k=0,1}=\alpha_0$, $\lambda_{k>0,-1}=\beta_{k+}$, $\lambda_{k<0,-1}=\beta_{k-}$, $\lambda_{k=0,-1}=\beta_0$, and $\lambda_{k,0}=a^{(a)}_{kB}$, and

$$\alpha_{k\pm}=\frac{1}{2}[1+J_k/(2\mu)]^{1/4}\left[\left(1+\frac{1}{\sqrt{1+J_k/(2\mu)}}\right)\Delta_{k\pm} \pm\left(1-\frac{1}{\sqrt{1+J_k/(2\mu)}}\right)\Delta^\dagger_{k\pm}\right], \quad (14)$$

$$\beta_{k\pm}=\frac{1}{2}[1-J_k/(2\mu)]^{1/4}\left[\left(1+\frac{1}{\sqrt{1-J_k/(2\mu)}}\right)\Theta_{k\pm} \pm\left(1-\frac{1}{\sqrt{1-J_k/(2\mu)}}\right)\Theta^\dagger_{k\pm}\right], \quad (15)$$

$$\alpha_0=\frac{1}{2}[1+J_0/(2\mu)]^{1/4}\left[\left(1+\frac{1}{\sqrt{1+J_0/(2\mu)}}\right)\psi_0 +\left(1-\frac{1}{\sqrt{1+J_0/(2\mu)}}\right)\psi^\dagger_0\right] - \frac{h}{2\sqrt{2}\mu}\sqrt{N/3}\left(\frac{2\mu}{g}\right)^{1/4}\left[\frac{1+\sqrt{2}/2}{(1+J_0/(2\mu))^{3/4}}\right], \quad (16)$$

$$\beta_0=\frac{1}{2}[1-J_0/(2\mu)]^{1/4}\left[\left(1+\frac{1}{\sqrt{1-J_0/(2\mu)}}\right)\phi_0 +\left(1-\frac{1}{\sqrt{1-J_0/(2\mu)}}\right)\phi^\dagger_0\right] + \frac{h}{2\sqrt{2}\mu}\sqrt{N/3}\left(\frac{2\mu}{g}\right)^{1/4}\left(\frac{1-\sqrt{2}/2}{(1-J_0/(2\mu))^{3/4}}\right). \quad (17)$$

The three eigenfrequencies read

$$\omega_{k,m}=\sqrt{2g\mu+gJ_{k,m}}, \quad m=0,\pm1, \quad (18)$$

where $J_{k,m}=2\sqrt{2}mJ\cos(k/2)$ and $J_k=J_{k,m=1}$ (see Fig. 2). Notice that two eigenfrequencies are dispersive ($m=\pm1$) and merely represent the Fourier transform of the linear AF spherical model with effective AF coupling $J\to\sqrt{2}J$ and number of sites given by $2N/3$, whereas the flatband ($m=0$) arises due to the AB_2 chain topology. The $k\to0$ expansion of the dispersive modes provides $\omega_{k,\pm1}=A_\pm\mp B_\pm k^2$, with $A_\pm$ and $B_\pm$ positive and the k^2 dependence typical of the magnon spectrum associated with the ground-state long-range ferrimagnetism present along with a constant term. Moreover, all modes are gapped for any finite g and nullify for $g=0$.

The diagonal Hamiltonian (13) allows us to obtain the quantum thermal averages in the canonical ensemble using the density operator

$$\hat{\rho}=\frac{e^{-\beta H}}{\mathrm{Tr}(e^{-\beta H})}=\prod_{k,m}[(1+e^{-\beta\omega_{k,m}})e^{-\beta\omega_{k,m}\lambda^\dagger_{k,m}\lambda_{k,m}}], \quad (19)$$

where a quantum thermal average is indicated by $\langle\cdots\rangle=\mathrm{Tr}(\hat{\rho}\cdots)$, and $\beta=1/T$. Single- and two-operator averages result in

$$\langle\lambda_{k,m}\rangle=\langle\lambda^\dagger_{k,m}\rangle=0 \quad (20)$$

and

$$\langle\lambda_{k,m}\lambda_{p,n}\rangle=0, \quad \langle\lambda^\dagger_{k,m}\lambda_{p,n}\rangle=\frac{\delta_{k,p}\delta_{m,n}}{e^{\beta\omega_{k,m}}-1}. \quad (21)$$

The Helmholtz free energy $F=U-TS$, with $U=\langle H\rangle$ and $S=-\langle\ln\hat{\rho}\rangle$, is then given by

$$F=T\sum_{k,m}\ln\left[2\sinh\left(\frac{1}{2}\beta\omega_{k,m}\right)\right]-\frac{N}{3}\left(\frac{h^2(1+\sqrt{2}/2)^2}{4(\mu+\sqrt{2}J)}+\frac{h^2(1-\sqrt{2}/2)^2}{4(\mu-\sqrt{2}J)}\right)-\mu\frac{N}{4}, \quad (22)$$

which includes a free bosonic term plus additional ones due to the magnetic energy and the chemical potential.

We can also express the spherical restriction, Eq. (1), as an equation for the chemical potential from the condition $\partial F/\partial\mu=0$:

$$\frac{h^2(1+\sqrt{2}/2)^2}{4(\mu+\sqrt{2}J)^2}+\frac{h^2(1-\sqrt{2}/2)^2}{4(\mu-\sqrt{2}J)^2}+\frac{3}{N}\sum_{k,m}\frac{g}{2\omega_{k,m}}\coth\left(\frac{1}{2}\beta\omega_{k,m}\right) =\frac{3}{4}. \quad (23)$$

In the Appendix we detail the continuous $N\gg1$ calculation of Eq. (23).

III. LOCAL SPIN AVERAGES, CELL MAGNETIZATION, AND SUSCEPTIBILITY

The spin variables Eq. (4) can be expressed, after the Bogoliubov transformations Eqs. (14)–(18) and auxiliary definitions Eqs. (7)–(12), as follows:

$$S_{iA} = \frac{\sqrt{2}}{2}\left(\frac{g}{2\mu}\right)^{1/4}\sqrt{3/N}\sum_{k>0}(f_k^a A_k^{(1)} + f_k^b B_k^{(1)} + \text{H.c.}) + \frac{1}{2}\left(\frac{g}{2\mu}\right)^{1/4}\sqrt{3/N}(f_0^{(a)}\alpha_0 + f_0^{(b)}\beta_0 + \text{H.c.}) + \frac{\sqrt{2}}{2}\left(\frac{h(1+\sqrt{2}/2)}{2(\mu+\sqrt{2}J)} - \frac{h(1-\sqrt{2}/2)}{2(\mu-\sqrt{2}J)}\right), \quad (24)$$

$$S_{iB\sigma} = \frac{\sigma}{2}\sqrt{3/N}\left(\frac{g}{2\mu}\right)^{1/4}\sum_{k}(e^{ikx_i}a_{kB}^{(a)} + \text{H.c.}) + \frac{1}{2}\left(\frac{g}{2\mu}\right)^{1/4}\sqrt{3/N}\sum_{k>0}(f_k^{(a)}A_k^{(2)} - f_k^{(b)}B_k^{(2)} + \text{H.c.}) + \frac{\sqrt{2}}{4}\left(\frac{g}{2\mu}\right)^{1/4}\sqrt{3/N}(f_0^{(a)}\alpha_0 - f_0^{(b)}\beta_0 + \text{H.c.}) + \frac{1}{2}\left[\frac{h(1+\sqrt{2}/2)}{2(\mu+\sqrt{2}J)} + \frac{h(1-\sqrt{2}/2)}{2(\mu-\sqrt{2}J)}\right], \quad (25)$$

where $\sigma = +1(-1)$ for B_1 (B_2) sites,

$$A_k^{(1)} = \cos(kx_i)\alpha_{k+} + i\sin(kx_i)\alpha_{k-},$$

$$A_k^{(2)} = \cos\left[k\left(x_i + \tfrac{1}{2}\right)\right]\alpha_{k+} + i\sin\left[k\left(x_i + \tfrac{1}{2}\right)\right]\alpha_{k-},$$

$$B_k^{(1)} = \cos(kx_i)\beta_{k+} + i\sin(kx_i)\beta_{k-},$$

$$B_k^{(2)} = \cos\left[k\left(x_i + \tfrac{1}{2}\right)\right]\beta_{k+} + i\sin\left[k\left(x_i + \tfrac{1}{2}\right)\right]\beta_{k-},$$

$$f_k^{(a)} = [1 + J_k/(2\mu)]^{-1/4},$$

$$f_k^{(b)} = [1 - J_k/(2\mu)]^{-1/4},$$

$$f_0^{(a)} = f_{k=0}^a,$$

and

$$f_0^{(b)} = f_{k=0}^b.$$

By taking quantum thermal averages, Eqs. (20) and (21), we obtain

$$\langle S_A\rangle = \frac{\sqrt{2}}{2}\left(\frac{h(1+\sqrt{2}/2)}{2(\mu+\sqrt{2}J)} - \frac{h(1-\sqrt{2}/2)}{2(\mu-\sqrt{2}J)}\right), \quad (26)$$

$$\langle S_B\rangle = \frac{1}{2}\left(\frac{h(1+\sqrt{2}/2)}{2(\mu+\sqrt{2}J)} + \frac{h(1-\sqrt{2}/2)}{2(\mu-\sqrt{2}J)}\right), \quad (27)$$

$$M_{\text{cell}} = \left(\frac{h(1+\sqrt{2}/2)^2}{2(\mu+\sqrt{2}J)} + \frac{h(1-\sqrt{2}/2)^2}{2(\mu-\sqrt{2}J)}\right), \quad (28)$$

where $\langle S_A\rangle \equiv \langle S_{iA}\rangle$, $\langle S_B\rangle \equiv \langle S_{iB_{1,2}}\rangle$, and $M_{\text{cell}} = \langle S_A\rangle + 2\langle S_B\rangle$.

First we notice that, although the field-induced magnetization per cell M_{cell} displays a quantum paramagnetic behavior for any finite g and T [see Fig. 3(a)], the spins at sites A and B could have different orientations as the values of g, T, h change and modify the value of μ through the spherical restriction, Eq. (A7), as seen in Fig. 3(b). Indeed, for special regions of the parameter space $\{g, T, h\}$, with finite h, spins at sites A point antiparallel with respect to those at sites $B_{1,2}$, thus giving rise to a field-induced short-range ferrimagnetism [Fig. 3(b)] and to a rapid increase of M_{cell} for very low fields [inset of Fig. 3(a)]. This short-range order, due to the AF interactions and the AB_2 topology, is destroyed for large values of g, T, or h, giving rise to standard paramagnetic behavior. Indeed, as the field increases, $\langle S_A\rangle$ is reversed after its minimum is reached, as shown in Fig. 3(b). It is interesting to notice that the value in which the spins at sites A reverse its signal ($h \approx 2.11J$ for $g = 0.05J$ and $T = 0.05J$) is compatible in magnitude with the values where the signal of spins at sites A is reversed in the AB_2 Ising and quantum Heisenberg models.[20,22] The surface that separates the regions $\langle S_A\rangle > 0$ and $\langle S_A\rangle < 0$ ($\langle S_B\rangle > 0$ and $h \neq 0$ in both cases) is obtained from Eqs. (A7) and (26) by requiring that $\langle S_A\rangle = 0$, i.e., $\mu = 2J$:

$$2A_0\left(\frac{4J}{T}, \frac{2\sqrt{2}J}{T}, \frac{g}{4T}\right) + B_0\left(\frac{4J}{T}, \frac{g}{4T}\right) + \frac{h^2}{4J^2}\frac{(1+\sqrt{2}/2)^2}{(2+\sqrt{2})^2} + \frac{h^2}{4J^2}\frac{(1-\sqrt{2}/2)^2}{(2-\sqrt{2})^2} = \frac{3}{4}. \quad (29)$$

On the other hand, after a maximum in $\langle S_B\rangle$ is achieved, $\langle S_A\rangle = \langle S_B\rangle \to 1/2$ and $M_{\text{cell}} \to 3/2$ in the asymptotic $h \gg \{J, g, T\}$ saturation limit, as expected (see Fig. 3). One should also notice that $\langle S_B\rangle > 1/2$ in the maximum, a result not incompatible with the spherical model, since the spherical restriction Eq. (1) applies to the *sum* of all expectation values $\langle S_{i\alpha}^2\rangle$ and, as already mentioned, the expected values

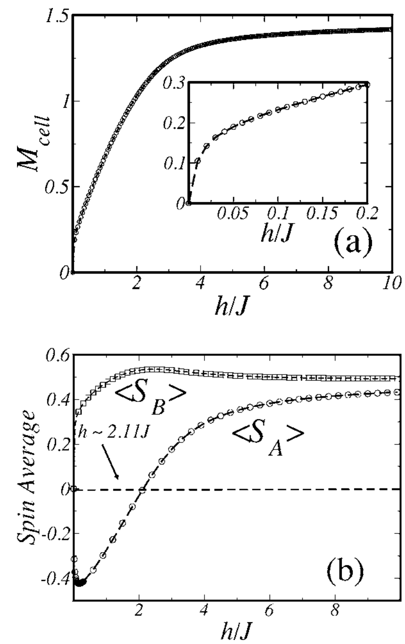

FIG. 3. (a) Cell magnetization and (b) spin averages at sites A (-○-) and B (-□-) as functions of h/J for $g = 0.05J$ and $T = 0.05J$. Inset of (a): very-low-field regime.

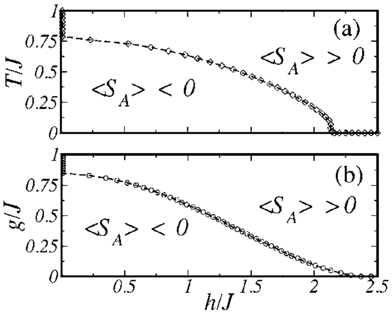

FIG. 4. Phase diagrams of the surface $\langle S_A\rangle=0$ that delimits the change of signal of spins at sites A for $\mu=2J$: (a) T/J as a function of h/J for $g=0.05J$ and (b) g/J as a function of h/J for $T=0.05J$.

of the spin operators $S_{i\alpha}$ may vary continuously, with no upper and lower bounds, differently from the usual quantum-mechanical spins. Therefore, it is actually possible to find solutions with $\langle S_B^2\rangle > 1/4$, provided that $\langle S_A^2\rangle < 1/4$ so to satisfy Eq. (1).

The phase diagrams displayed in Fig. 4 show that the behavior of the phase boundary near $h=0$ is essentially determined by the existence or not of the zero of $\langle S_A\rangle$ at finite h, shown in Fig. 3(b). For sufficiently intense thermal (quantum) disorder, Fig. 4(a) [Fig. 4(b)], the field-induced short-range ferrimagnetism, with $\langle S_A\rangle<0$ and $\langle S_B\rangle>0$, does not stabilize and the system presents a disordered quantum paramagnetic state, with both $\langle S_A\rangle>0$ and $\langle S_B\rangle>0$ in a field, in which case the finite-h zero of $\langle S_A\rangle$ no longer exists.

Another remarkable point is that Eqs. (26)–(28) have poles only at $\mu=-\sqrt{2}J$ and $\sqrt{2}J$; the former is unphysical and the latter occurs only for the case $g=T=h=0$. Nontrivial solutions of Eq. (A7) exist only for $\mu>\sqrt{2}J$. This indicates that the only critical point $g=T=h=0$ of the quantum AB_2 spherical model excludes the possibility of a zero-field thermal ($T\neq 0$) or quantum ($g\neq 0$) spontaneous symmetry breaking from a paramagnetic to a ferrimagnetic long-range ordered state at finite T or g, respectively. Further, for $g=T=h=0$ the average spins and the cell magnetization assume the following finite values, consistent with the spherical constraint, Eq. (1):

$$\langle S_A\rangle = -\sqrt{\frac{3}{8}},\quad \langle S_B\rangle = \sqrt{\frac{3}{16}},\quad M_{\mathrm{cell}} = (\sqrt{2}-1)\sqrt{\frac{3}{8}}, \tag{30}$$

so that the average spin of a unit cell is less than 1/2. In contrast, it is interesting to notice that the AB_2 Hubbard model, as well as its strong-coupling half-filled limit, the quantum AF AB_2 Heisenberg model, present zero-field ferrimagnetic ground state with $M_{\mathrm{cell}}=1/2$, due to a theorem by Lieb.[20,21,25]

From Eq. (28), the magnetic susceptibility per cell, $\chi_{\mathrm{cell}}=\partial M_{\mathrm{cell}}/\partial h$, is given by

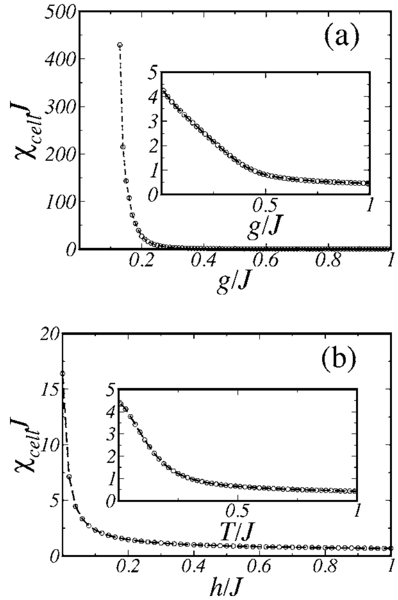

FIG. 5. (a) Cell susceptibility times J as function of (a) g/J for $T=h=0$ (inset: $T=0.05J$ and $h=0.05J$) and (b) h/J for $g=0.05J$ and $T=0.05J$ (inset: as function of T/J for $g=0.05J$ and $h=0.05J$).

$$\chi_{\mathrm{cell}} = \frac{1}{J}\frac{\sqrt{2}}{4}\left[\left(\frac{(1+\sqrt{2}/2)^2}{\mu/(\sqrt{2}J)+1} + \frac{(1-\sqrt{2}/2)^2}{\mu/(\sqrt{2}J)-1}\right) - \frac{h}{4J}\left(\frac{(1+\sqrt{2}/2)^2}{[\mu/(\sqrt{2}J)+1]^2} + \frac{(1-\sqrt{2}/2)^2}{[\mu/(\sqrt{2}J)-1]^2}\right)\frac{\partial\mu}{\partial h}\right], \tag{31}$$

which is finite for all values of $\{g,T,h\}$, except for the singular point $g=T=h=0$, where the pole $\mu=\sqrt{2}J$ is achieved. By solving the spherical restriction Eq. (A7) near this pole, with the use of either Eq. (A12) or Eq. (A13), we obtain three distinct behaviors of χ_{cell} depending on the path chosen:

$$\chi_{\mathrm{cell}} \sim \frac{3(\sqrt{2}-1)}{512J}\exp\left(\frac{3\pi}{2}\sqrt{\frac{\sqrt{2}J}{g}}\right),\quad T=h=0,\quad (g/J)\to 0, \tag{32}$$

$$\chi_{\mathrm{cell}} \sim \frac{(2-\sqrt{2})(16-\sqrt{18-12\sqrt{2}})\sqrt{9+6\sqrt{2}}}{12h},\qquad g=T=0,\quad (h/J)\to 0, \tag{33}$$

and

$$\chi_{\mathrm{cell}} \sim \frac{(27\sqrt{2}-36)}{32}\frac{J}{T^2},\quad g=h=0,\quad (T/J)\to 0. \tag{34}$$

Notice in Eq. (32) the nonanalytical divergence associated with the essential singularity in χ_{cell} due to quantum fluctuations as $(g/J)\to 0$, with $T=h=0$ [see Fig. 5(a)]. In this case, the introduction of thermal flucutuations and/or magnetic field causes χ_{cell} to achieve a finite maximum at $g=0$ [see inset of Fig. 5(a)]. A similar finite maximum in χ_{cell} is in-

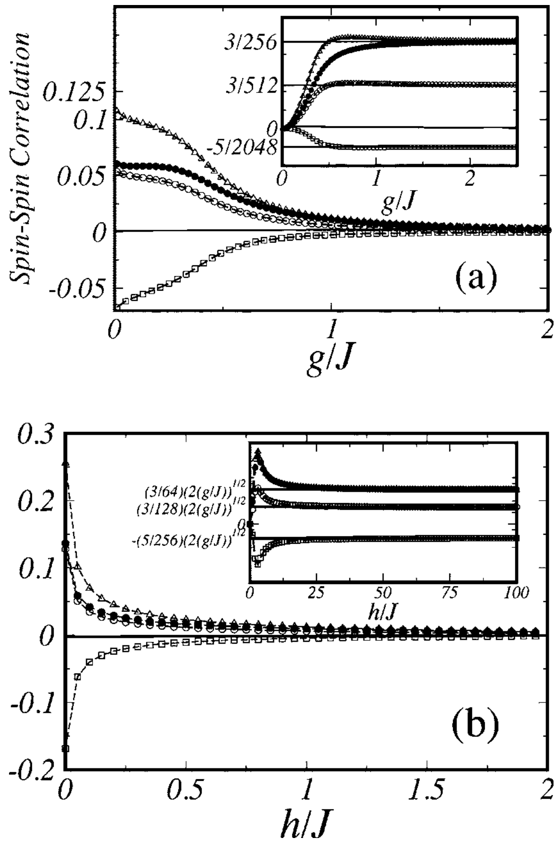

FIG. 6. Correlation functions between spins B_1 and B_2 at the same cell (-●-) and between spins of first-neighbor cells [sites A (-△-), $B_{1,2}$ (-○-), and A and $B_{1,2}$ (-□-)]: (a) as function of g/J for $T=0.05J$ and $h=0.05J$; (b) as function of h/J for $g=0.05J$ and $T=0.05J$. The insets show the convergence to the asymptotic limits, respectively multiplied by (a): $(g/J)^2$ (first three correlation functions) and $(g/J)^3$(last one); and (b): $(h/J)^{5/2}$ (first three correlation functions) and $(h/J)^{7/2}$ (last one).

duced by quantum and/or thermal fluctuations (quantum fluctuations and/or magnetic field) in the regime described by Eq. (33) [Eq. (34)], as shown in Fig. 5(b). This analysis confirms that the presence of magnetic field or quantum or thermal fluctuations destroys the ferrimagnetic long-range order, giving rise to a field-induced short-range order with large but finite χ_{cell} and a rapid increase of M_{cell} at very low fields, as shown in the inset of Fig. 3(a). We also remark that the power-law $1/T^2$ susceptibility decay as $(T/J)\to 0$, for $g=h=0$, Eq. (34), is also shared by the classical[2,26] and quantum[15] linear spherical models, classical[27] and quantum ferromagnetic[28] Heisenberg chains, as well as by the quantum[21] and classical[22] AB_2 AF Heisenberg models.

Further, the standard paramagnetic behavior of χ_{cell} is approached for distinct parameter limits as follows:

$$\chi_{\text{cell}} \sim \frac{25J^2}{3h^3}, \quad h \gg \{J,g,T\}, \tag{35}$$

$$\chi_{\text{cell}} \sim \frac{3}{4g}, \quad g \gg \{J,T,h\}, \tag{36}$$

and

$$\chi_{\text{cell}} \sim \frac{3}{4T}, \quad T \gg \{J,g,h\}, \tag{37}$$

where the expected Curie-like behavior is observed due to either thermal or quantum fluctuations.

IV. CORRELATION FUNCTIONS

Using Eqs. (20), (21), and (24), the correlation between spins at sites A of cells i and j yields

$$\langle S_{iA}S_{jA}\rangle - \langle S_{iA}\rangle\langle S_{jA}\rangle = \frac{1}{2}\sum_k \left[\frac{g}{2\omega_{k,+}}\coth\left(\frac{1}{2}\beta\omega_{k,+}\right) + \frac{g}{2\omega_{k-}}\coth\left(\frac{1}{2}\beta\omega_{k,-}\right)\right]\cos[2k(j-i)], \tag{38}$$

which, with the use of Eq. (A1), can be written as

$$\langle S_{iA}S_{jA}\rangle - \langle S_{iA}\rangle\langle S_{jA}\rangle = \int_{-\pi}^{\pi}\frac{d\theta}{2\pi}\cos[2(j-i)\theta]\frac{g}{2\omega(\theta)}\coth\left(\frac{1}{2}\beta\omega(\theta)\right). \tag{39}$$

In addition, from Eqs. (A5) and (A6) we can write

$$\langle S_{iA}S_{jA}\rangle - \langle S_{iA}\rangle\langle S_{jA}\rangle = \frac{1+\delta_{ij}}{2}A_{2(j-i)}\left(\frac{2\mu}{T},\frac{2\sqrt{2}J}{T},\frac{g}{4T}\right). \tag{40}$$

Following similar arguments, we obtain the correlation between spins at sites B of same type, i.e., sites B_1 of cells i and j, or sites B_2 of cells i and j:

$$\begin{aligned}\langle S_{iB_{1,2}}S_{jB_{1,2}}\rangle - \langle S_{iB_{1,2}}\rangle\langle S_{jB_{1,2}}\rangle &= \frac{1}{2}\int_{-\pi}^{\pi}\frac{d\theta}{2\pi}\cos[2(j-i)\theta]\frac{g}{2\omega(\theta)}\coth\left(\frac{1}{2}\beta\omega(\theta)\right) + \frac{\delta_{ij}}{2}\frac{g}{2\omega_0}\coth\left(\frac{1}{2}\beta\omega_0\right)\\ &= \frac{1+\delta_{ij}}{4}A_{2(j-i)}\left(\frac{2\mu}{T},\frac{2\sqrt{2}J}{T},\frac{g}{4T}\right) + \frac{\delta_{ij}}{2}B_0\left(\frac{2\mu}{T},\frac{g}{4T}\right),\end{aligned} \tag{41}$$

the correlation between spins at sites B_1 of cell i and spins at sites B_2 of cell j,

$$\begin{aligned}\langle S_{iB_1}S_{jB_2}\rangle - \langle S_{iB_1}\rangle\langle S_{jB_2}\rangle &= \frac{1}{2}\int_{-\pi}^{\pi}\frac{d\theta}{2\pi}\cos[2(j-i)\theta]\frac{g}{2\omega(\theta)}\coth\left(\frac{1}{2}\beta\omega(\theta)\right) - \frac{\delta_{ij}}{2}\frac{g}{2\omega_0}\coth\left(\frac{1}{2}\beta\omega_0\right)\\ &= \frac{1+\delta_{ij}}{4}A_{2(j-i)}\left(\frac{2\mu}{T},\frac{2\sqrt{2}J}{T},\frac{g}{4T}\right) - \frac{\delta_{ij}}{2}B_0\left(\frac{2\mu}{T},\frac{g}{4T}\right),\end{aligned} \tag{42}$$

and the correlation between spins at sites A and $B_{1,2}$ of cells i and j, respectively,

$$\langle S_{iA}S_{jB_{1,2}}\rangle - \langle S_{iA}\rangle\langle S_{jB_{1,2}}\rangle = \frac{\sqrt{2}}{2}\int_{-\pi}^{\pi}\frac{d\theta}{2\pi}\cos\{[2(j-i)+1]\theta\}\frac{g}{2\omega(\theta)}\coth\left(\frac{1}{2}\beta\omega(\theta)\right) = \frac{\sqrt{2}}{4}A_{2(j-i)+1}\left(\frac{2\mu}{T},\frac{2\sqrt{2}J}{T},\frac{g}{4T}\right). \quad (43)$$

Notice that the spin-spin correlation functions behave in a way that confirms the ferrimagnetic short-range order induced by the magnetic field and also manifested in the previous analysis of magnetization and susceptibility. As seen in Fig. 6 for spins at first-neighbor cells, sites A and $B_{1,2}$ have a negative correlation function which tends to zero for $g \gg \{T,h\}$ [Fig. 6(a)] and $h \gg \{g,T\}$ [Fig. 6(b)]. In the latter, for $h \gg \{g,T\}$ the spins tend to their saturation values as, e.g., $\langle S_{iA}S_{jA}\rangle \to \langle S_{iA}\rangle\langle S_{jA}\rangle = (1/2)^2$, and similar results for the other correlation functions, thus leading to a null spin-spin correlation at the high-h paramagnetic limit.

These limiting results can also be analytically probed by considering the asymptotic behavior of Eqs. (A10) and (A11) in Eqs. (40)–(43). For $g \gg \{J,T,h\}$ or $T \gg \{J,g,h\}$ we obtain

$$A_n \sim \begin{cases} (-1)^n[(2-\delta_{n,0})/4](\sqrt{2}J/4g)^n[(2n-1)!!/(2n)!!], & g \gg \{J,T,h\}, \\ (-1)^n[(2-\delta_{n,0})/4](\sqrt{2}J/4T)^n, & T \gg \{J,g,h\}, \end{cases}$$

$$B_0 \sim A_0 - A_2, \quad g \gg \{J,T,h\} \quad \text{or} \quad T \gg \{J,g,h\}, \quad (44)$$

thus revealing the asymptotic power-law decay of the correlation functions with spin distance (index n) and large g or T. In particular, as shown in Fig. 6(a), by applying Eq. (44) in Eqs. (40)–(43), the $g \gg \{J,T,h\}$ asymptotic limit of the correlation between spins B_1 and B_2 at the same cell reads $\langle S_{iB_1}S_{iB_2}\rangle - \langle S_{iB_1}\rangle\langle S_{iB_2}\rangle = (A_0-B_0)/2 \sim (3J^2)/(256g^2)$, whereas spin-spin correlations in first-neighbor cells are $\langle S_{iA}S_{(i+1)A}\rangle - \langle S_{iA}\rangle\langle S_{(i+1)A}\rangle = A_2/2 \sim (3J^2/256g^2)$, $\langle S_{iB_{1,2}}S_{(i+1)B_{1,2}}\rangle - \langle S_{iB_{1,2}}\rangle\langle S_{(i+1)B_{1,2}}\rangle = (A_2/4) \sim (3J^2)/(512g^2)$, and $\langle S_{iA}S_{(i+1)B_{1,2}}\rangle - \langle S_{iA}\rangle\langle S_{(i+1)B_{1,2}}\rangle = (\sqrt{2}/4)A_3 \sim (-5J^3)/(2048g^3)$. These asymptotic results are confirmed by the convergence analysis indicated in the inset of Fig. 6(a).

On the other hand, for $h \gg \{J,T,h\}$,

$$A_n \sim \begin{cases} (-1)^n[(2-\delta_{n,0})/2](T/h)(\sqrt{2}J/2h)^n, & g=0, \quad h \gg \{J,g,T\}, \\ (-1)^n[(2-\delta_{n,0})/4](\sqrt{2gh}/h)(\sqrt{2}J/2h)^n[(2n-1)!!/(2n)!!], & g \neq 0, \quad h \gg \{J,g,T\}, \end{cases}$$

$$B_0 \sim A_0 - A_2, \quad h \gg \{J,g,T\}, \quad (45)$$

which leads to $\langle S_{iB_1}S_{iB_2}\rangle - \langle S_{iB_1}\rangle\langle S_{iB_2}\rangle = (A_0-B_0)/2 \sim (3\sqrt{2gh}J^2)/(64h^3)$, $\langle S_{iA}S_{(i+1)A}\rangle - \langle S_{iA}\rangle\langle S_{(i+1)A}\rangle = A_2/2 \sim (3\sqrt{2gh}J^2/64h^3)$, $\langle S_{iB_1}S_{(i+1)B_2}\rangle - \langle S_{iB_{1,2}}\rangle\langle S_{(i+1)B_{1,2}}\rangle = (A_2/4) \sim (3\sqrt{2gh}J^2)/(128h^3)$, and $\langle S_{iA}S_{(i+1)B_{1,2}}\rangle - \langle S_{iA}\rangle\langle S_{(i+1)B_{1,2}}\rangle = (\sqrt{2}/4)A_3 \sim (-5\sqrt{2gh}J^3)/(256h^4)$, as shown in Fig. 6(b). These asymptotic results are also confirmed by the rather slow convergence in low fields, as displayed in the inset of Fig. 6(b).

For the analysis of the critical point $g=T=h=0$ we use the special limits of Eq. (A10). For $g=0$,

$$A_n = 2(-1)^n A_0\left(\frac{\mu}{\sqrt{2}J} - \sqrt{\frac{\mu^2}{2J^2}-1}\right)^n; \quad (46)$$

for $T \to 0$, following the same arguments that led to Eq. (A13), we obtain

$$A_n = 2(-1)^n\frac{\sqrt{g}}{\pi}\int_0^\infty dx\frac{\{(2\mu+x^2)/(2\sqrt{2}J) - \sqrt{[(2\mu+x^2)/(8J^2)]^2-1}\}^n}{\sqrt{(2\mu+x^2)^2-8J^2}}. \quad (47)$$

The point $g=T=h=0$ can therefore be accessed by using either Eq. (46) or Eq. (47), although the calculation in the latter case needs a steepest descent analysis of the integral. For both cases we obtain $A_n = \frac{3}{4}(-1)^n$, and all correlations are distance independent, assuming values consistent with the spherical constraint

$$\langle S_{iA}S_{jA}\rangle = \frac{3}{8}, \quad \langle S_{iB_{1,2}}S_{jB_{1,2}}\rangle = \frac{3}{16}, \quad \langle S_{iA}S_{jB_{1,2}}\rangle = -\frac{3\sqrt{2}}{16}. \quad (48)$$

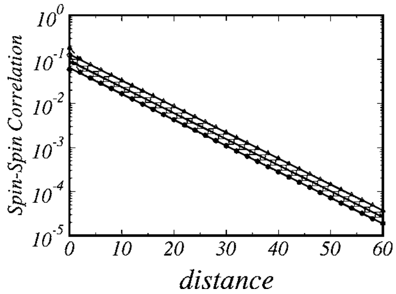

FIG. 7. Absolute values of spin-spin correlation between sites A (-△-), sites $B_{1,2}$ (-◯-), sites B_1 and B_2 (-•-), and sites A and $B_{1,2}$ (-□-) as function of distance (in units of $d/2$), for $g=0.05J$, $T=0.05J$, and $h=0.05J$. The straight lines indicate the exponential decay.

It is also relevant to perceive that the sum of all correlations is not proportional to the susceptibility, Eq. (31). This feature also happens in the classical mean spherical model.[29] Here, however, the reason is based on the fact that we have to take first the quantum thermal averages in order to get the magnetization and then obtain the susceptibility from derivation in a field; the order of these two operations cannot be exchanged since $[P_{i\alpha}^2, S_{j\beta}]=-2\delta_{ij}\delta_{\alpha,\beta}P_{i\alpha}$ in the Hamiltonian, Eq. (3), which implies $\partial e^{-\beta H}/\partial h \neq -\beta e^{-\beta H}\partial H/\partial h$.

For all cases, excluding the point $g=T=h=0$, the correlations functions decay exponentially with distance, as expected for a system without thermal ($T\neq 0$) or quantum ($g \neq 0$) phase transition (see Fig. 7). In fact, this can also be inferred from the analysis of the correlation length ξ (in units of d). By writing $A_n=(-1)^n(2T/\sqrt{4\mu^2-8J^2})\exp(-n/2\xi)$, we identify, from Eq. (A10) with $s=0$ and $n\gg 1$:

$$\xi = -\frac{1}{2\ln[\mu/(\sqrt{2}J)-\sqrt{(\mu^2/2J^2)-1}]}. \tag{49}$$

The above formula can also be obtained for the case $T\to 0$ from a careful steepest descent analysis of Eq. (47). From Eq. (49) one can see that the ξ diverges as the point $g=T=h=0$, corresponding to $\mu=\sqrt{2}J$, is approached. However, this divergence is strongly dependent on the path chosen:

$$\xi \sim \frac{\sqrt{2}}{16}\exp\left(\frac{3\pi}{4}\sqrt{\frac{\sqrt{2}J}{g}}\right), \quad T=h=0, \quad (g/J)\to 0, \tag{50}$$

$$\xi \sim 2\sqrt{9+6\sqrt{2}}\sqrt{\frac{J}{h}}, \quad g=T=0, \quad (h/J)\to 0, \tag{51}$$

and

$$\xi \sim \frac{3\sqrt{2}J}{4T}, \quad g=h=0, \quad (T/J)\to 0. \tag{52}$$

Notice the consistency between Eqs. (32)–(34) for $\chi_{\rm cell}$ and Eqs. (50)–(52) above. In particular, one observes that $\chi_{\rm cell}\sim\xi^2$ in all cases.

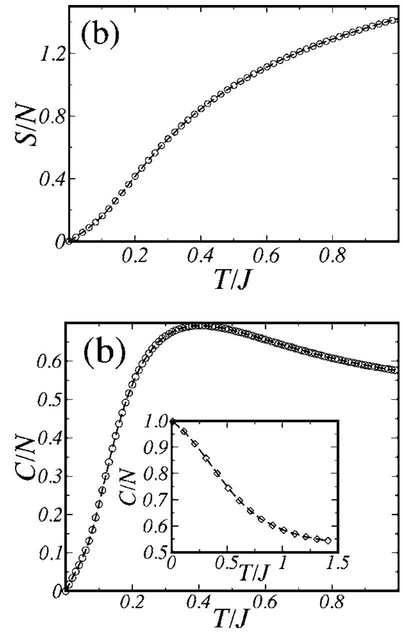

FIG. 8. (a) Entropy per site and (b) specific heat per site as function of T for $g=0.1J$ and $h=0$ (inset: $g=h=0$).

V. ENTROPY AND SPECIFIC HEAT

The entropy of the system is calculated from Eq. (22) as follows:

$$S = -\frac{\partial F}{\partial T} = \sum_{k,m}\left(\frac{\beta\omega_{k,m}}{\exp(\beta\omega_{k,m})-1} - \ln[1-\exp(-\beta\omega_{k,m})]\right). \tag{53}$$

From the equation above, the specific heat is readily obtained:

$$C = T\frac{\partial S}{\partial T} = \sum_{k,m}\frac{(\beta\omega_{k,m})^2\exp(\beta\omega_{k,m})}{[\exp(\beta\omega_{k,m})-1]^2}\left(1-\frac{g}{\omega_{k,m}^2}T\frac{\partial\mu}{\partial T}\right), \tag{54}$$

as displayed in Fig. 8. Note that the above expressions are formally similar to those of a free bosonic system, except for the explicit g dependence in Eq. (54) characteristic of the spherical model, although the chemical potential is here a special function of g, T, and h through the spherical condition, Eq. (A7). Interestingly, the $\partial\mu/\partial T$ term is also present in the classical spherical model.[2]

Notice that for $g\neq 0$ the well-known[2] drawback (finite C and diverging S) of classical spherical models concerning the third law of thermodynamics as $T\to 0$ is absent in Eqs. (53) and (54). However, by taking $g\to 0$ and $h=0$ in Eq. (53), this anomaly appears as

$$\begin{aligned} S &\sim S_{div} + S_{div}^{BK} - \frac{1}{2}\sum_{k,m}\ln\frac{(2\mu+J_{k,m})}{2\sqrt{2}J} + N \\ &= S_{div} + S_{div}^{BK} - \frac{1}{2}\left[2\frac{N}{3}\ln\left(\frac{\mu}{\sqrt{2}J}-\sqrt{\frac{\mu^2}{2J^2}-1}\right)+\frac{N}{3}\ln\frac{\mu}{\sqrt{2}J}\right] \\ &\quad + N, \quad N\gg 1, \end{aligned} \tag{55}$$

where $S_{div}=(N/2)\ln(T/g)$ and $S_{div}^{BK}=(N/2)\ln[T/(2\sqrt{2}J)]$. We note that the extra divergent term S_{div} is absent in the classical spherical model. By following the path $g=T$, with $T\to 0$, such term disappears and we obtain [see inset of Fig. 8(b)]

$$C = C^{BK} + \frac{N}{2}, \tag{56}$$

where the classical result[2] reads

$$C^{BK} = \frac{N}{2}\left(1 + 4K^2\frac{dz_s}{dK}\right), \tag{57}$$

with $K=J/8T$ and $z_s=\mu/J$.

For $T \ll \{J,g,h\}$ and nonzero g a steepest descent analysis of the continuum limit of Eqs. (53) and (54) leads to

$$\frac{S}{N} \sim \frac{1}{3}\left(\frac{\theta_l}{T}\right)\exp\left(-\frac{\theta_l}{T}\right) + \frac{2}{3}D\left(\frac{\theta_d}{T}\right)^{0.5}\exp\left(-\frac{\theta_d}{T}\right), \quad T \ll \{J,g,h\}, \tag{58}$$

$$\frac{C}{N} \sim \frac{1}{3}\left(\frac{\theta_l}{T}\right)^2\exp\left(-\frac{\theta_l}{T}\right) + \frac{2}{3}D\left(\frac{\theta_d}{T}\right)^{1.5}\exp\left(-\frac{\theta_d}{T}\right), \quad T \ll \{J,g,h\}, \tag{59}$$

where $\mu_0=\mu(g,T=0,h)$, $D=\sqrt{4\pi[\mu_0/(\sqrt{2}J)-1]}$, $\theta_l=\sqrt{2g\mu_0}$, and $\theta_d=\sqrt{2g(\mu_0-\sqrt{2}J)}$. The first exponential dependence in S and C above is due to the flat mode; the second is related to the gap of the dispersive modes, as shown in Fig. 2. In the second term of Eq. (59) the k-independent contribution in the low-k expansion for the dispersive eigenmodes $\omega_{k,\pm1}$, Eq. (18), leads to the exponential dependence multiplied by a $1/T^2$ prefactor (similar to Einstein's model); on the other hand, the k^2 term in that expansion multiplies a spin-wave-like $T^{0.5}$ factor, thus generating the overall $1/T^{1.5}$ dependence. On the other hand, for $T \gg \{J,g,h\}$ we have

$$\frac{S}{N} \sim \frac{1}{2}\ln\left(\frac{T}{4g}\right) + 1, \tag{60}$$

$$\frac{C}{N} \sim \frac{1}{2}. \tag{61}$$

We remark that the degrees of freedom associated with the canonical conjugate momentum $P_{i\alpha}$ do not add to the high-temperature specific heat due to the contribution of the g term in Eq. (54).

VI. CONCLUSIONS

We have studied a quantized version of the spherical spin model on the AB_2 chain, whose topology is of interest in the context of ferrimagnetic polymers and oxocuprates. We have focused attention on the effects of quantum (g) and thermal (T) fluctuations, under an external magnetic field (h), in observables such as local spin averages, cell magnetization and susceptibility, correlation functions, entropy and specific heat.

The quantum AB_2 spherical model goes through a spontaneous symmetry breaking to a state with ferrimagnetic long-range order at the only critical point $g=T=h=0$. The correlation functions for $g=T=h=0$ are distance independent and assume finite values consistent with the spherical restriction. The approach to the critical point is characterized through several paths in the $\{g,T,h\}$ parameter space: for $T=h=0$ and $(g/J)\to 0$ the susceptibility $\chi_{\rm cell}$ (and correlation length ξ) exhibits an essential singularity, i.e., $\ln \chi_{\rm cell} \sim 1/\sqrt{g}$, whereas for $g=T=0$ and $(h/J)\to 0$ or for $g=h=0$ and $(T/J)\to 0$ they display power-law decays with h and T, respectively: $\chi_{\rm cell}\sim 1/h$ and $\chi_{\rm cell}\sim 1/T^2$. In any path chosen the relation $\chi_{\rm cell}\sim \xi^2$ holds.

On the other hand, for any finite g, T, or h quantum and/or thermal fluctuations destroy the long-range order in the system. In this regime, the spins remain ferrimagnetically short-range ordered to some extent in the $\{g,T,h\}$ parameter space as a consequence of the AF interaction and the AB_2 topology. This field-induced quantum paramagnetic behavior is characterized by a rapid increase of the cell magnetization in very low fields. These results are confirmed by the analysis of the local spin averages and spin-spin correlation functions. The asymptotic limits of the correlation functions are also provided with respect to g, T, and h. Further, the analysis of the entropy and specific heat revealed that quantum fluctuations fix the well-known drawback of classical spherical models concerning the third law of thermodynamics.

ACKNOWLEDGMENTS

It is a pleasure to thank C. Vitoriano and R. R. Montenegro-Filho for helpful discussions. This work was partially supported by CNPq, CAPES, FINEP, and FACEPE (Brazilian agencies).

APPENDIX: CHEMICAL POTENTIAL CALCULATION IN THE $N \gg 1$ LIMIT

In order to obtain the chemical potential $\mu(g,T,h)$ from Eq. (23) in the $N\gg 1$ limit, we use the Euler-Maclaurin sum formula:

$$\sum_{k,m} \to \sum_m \frac{N}{3}\int_{-\pi}^{\pi}\frac{dk}{2\pi}, \quad N \gg 1, \tag{A1}$$

from which the last term in Eq. (23) becomes

$$\int_{-\pi}^{\pi}\frac{dk}{2\pi}\frac{g}{2\omega_{k,m}}\coth\left(\frac{1}{2}\beta\omega_{k,m}\right) = 2\int_{-\pi}^{\pi}\frac{d\theta}{2\pi}\frac{g}{2\omega(\theta)}\coth\left(\frac{1}{2}\beta\omega(\theta)\right) + \frac{g}{2\omega_0}\coth\left(\frac{1}{2}\beta\omega_0\right), \tag{A2}$$

with the two dispersive bands ($\omega_{k,\pm1}$) now represented by $\omega(\theta)=\sqrt{2g\mu+2\sqrt{2}gJ\cos\theta}$ and the flatband denoted by $\omega_0=\sqrt{2g\mu}$. Next, by considering the following function:

$$Y(a,b,c,\theta) = \frac{\sqrt{c}\coth[\sqrt{c(a+b\cos\theta)}]}{\sqrt{a+b\cos\theta}}, \quad \text{(A3)}$$

and its Fourier series

$$Y(a,b,c,\theta) = \sum_{n=0}^{\infty} A_n(a,b,c)\cos(n\theta), \quad \text{(A4)}$$

$$A_n(a,b,c) = (2-\delta_{n0})\int_{-\pi}^{\pi}\frac{d\theta}{2\pi}Y(a,b,c,\theta)\cos(n\theta), \quad \text{(A5)}$$

$$B_0(a,c) = Y(a,b=0,c,\theta), \quad \text{(A6)}$$

we can express Eq. (23), for $N \gg 1$, as

$$2A_0\left(\frac{2\mu}{T},\frac{2\sqrt{2}J}{T},\frac{g}{4T}\right) + B_0\left(\frac{2\mu}{T},\frac{g}{4T}\right) + \frac{h^2(1+\sqrt{2}/2)^2}{4(\mu+\sqrt{2}J)^2} + \frac{h^2(1-\sqrt{2}/2)^2}{4(\mu-\sqrt{2}J)^2} = \frac{3}{4}. \quad \text{(A7)}$$

The Fourier coefficients $A_n(a,b,c)$ can be evaluated using the partial fraction series of the hyperbolic cotangent:

$$\coth x = \frac{1}{x} + \sum_{s=1}^{\infty}\frac{2x}{x^2+s^2\pi^2}, \quad \text{(A8)}$$

and

$$\frac{1}{c+d\cos\theta} = \frac{1}{\sqrt{c^2-d^2}}\left(1+2\sum_{s=1}^{\infty}[(c/d) - \sqrt{(c/d)^2-1}]^s\cos(s\theta)\right), \quad c>d>0, \quad \text{(A9)}$$

so as to obtain

$$A_n(a,b,c) = (2-\delta_{n0})(-1)^n\sum_{s=-\infty}^{\infty}\frac{[(a_s/b)-\sqrt{(a_s/b)^2-1}]^n}{\sqrt{a_s^2-b^2}}, \quad \text{(A10)}$$

$$B_0(a,c) = \frac{1}{a} + 2\sum_{s=1}^{\infty}\frac{1}{a_s}, \quad a_s = a + \frac{s^2\pi^2}{c}. \quad \text{(A11)}$$

At this point we remark two important limits of A_0 and B_0: for $g=0$,

$$A_0 = \frac{T}{2\sqrt{\mu^2-2J^2}}, \quad B_0 = \frac{T}{2\mu}, \quad \text{(A12)}$$

and for $T\to 0$, we have $c=(g/4T)\to\infty$, so that $a_{s+1}-a_s\to 0$ and, in the continuum limit, the Euler-Maclaurin sum formula leads to

$$A_0 = \frac{\sqrt{g}}{\pi}\int_0^{\infty}\frac{dx}{\sqrt{(2\mu+x^2)^2-8J^2}}, \quad B_0 = \frac{g}{2\sqrt{2g\mu}}. \quad \text{(A13)}$$

*Electronic address: mario@lftc.ufpe.br
†Electronic address: mdcf@ufpe.br
‡Electronic address: ernesto@df.ufpe.br

[1] H. E. Stanley, Phys. Rev. **176**, 718 (1968); *Introduction to Phase Transitions and Critical Phenomena* (Oxford University Press, New York, 1971), p. 128, and references therein.
[2] T. H. Berlin and M. Kac, Phys. Rev. **86**, 821 (1952).
[3] B. S. Gourary and R. W. Hart, Phys. Rev. **95**, 676 (1954); W. K. Theumann, J. Chem. Phys. **51**, 3484 (1969); H. J. F. Knops, Phys. Rev. B **8**, 4209 (1973); W. K. Theumann, *ibid.* **15**, 3534 (1977).
[4] L. Kalok and L. C. de Menezes, Z. Phys. B **20**, 223 (1975); L. Kalok and G. Obermair, J. Phys. C **9**, 819 (1975).
[5] R. M. Hornereich, M. Luban, and S. Shtrikman, Physica A **86**, 465 (1977); C. S. O. Yokoi, M. D. Coutinho-Filho, and S. R. Salinas, Phys. Rev. B **24**, 4047 (1981).
[6] G. S. Joyce, in *Phase Trasitions and Critical Phenomena*, edited by C. Domb and M. S. Green (Academic, New York, 1972), Vol. 2, p. 375, and references therein.
[7] C. J. Thompson, *Classical Equilibrium Statistical Mechanics* (Clarendon Press, Oxford, 1988), p. 159, and references therein.
[8] A. C. Ribeiro Teixeira and D. A. Stariolo, Phys. Rev. E **70**, 016113 (2004).
[9] M. L. Lyra, M. D. Coutinho-Filho, and A. M. Nemirovsky, Phys. Rev. B **48**, 3755 (1993).
[10] A. M. Khorunzhy, B. A. Khoruzhenko, L. A. Pastur, and M. V. Scherbina, in *Phase Trasitions and Critical Phenomena*, edited by C. Domb and J. Lebowitz (Academic, New York, 1992), Vol. 15, p. 73, and references therein.
[11] J. M. Kosterlitz, D. J. Thouless, and R. C. Jones, Phys. Rev. Lett. **36**, 1217 (1976); A. Theumann, J. Phys. A **20**, 25 (1987); A. Jagannhathan, S. Eva, and J. Rudnick, *ibid.* **24**, 2193 (1991).
[12] M. Schwartz, Phys. Lett. **76A**, 408 (1980); J. F. Perez, W. F. Wreszinski, and J. L. Hemmen, J. Stat. Phys. **35**, 89 (1984); W. K. Theumann and J. F. Fontanari, *ibid.* **45**, 99 (1986); Physica A **149**, 341 (1988); W. F. Wreszinski and S. R. A. Salinas, *Disorder and Competition in Soluble Lattice Models* (World Scientific, Singapore, 1993), p. 35, and references therein; T. Vojta and M. Schreiber, Phys. Rev. B **50**, 1272 (1994).
[13] P. Shukla and S. Singh, Phys. Lett. **81A**, 477 (1981); T. K. Kopeć and K. D. Usadel, Phys. Rev. Lett. **78**, 1988 (1997); T. M. Nieuwenhuizen and F. Ritorti, Physica A **250**, 8 (1998); A. Crisanti and L. Leuzzi, Phys. Rev. Lett. **93**, 217203 (2004).
[14] T. M. Nieuwenhuizen, Phys. Rev. Lett. **74**, 4293 (1995).
[15] T. Vojta, Phys. Rev. B **53**, 710 (1996).
[16] T. Vojta and M. Schreiber, Phys. Rev. B **53**, 8211 (1996).
[17] R. Serral Gracià and T. M. Nieuwenhuizen, Phys. Rev. E **69**, 056119 (2004).

[18] See, e.g., J. Silvestre and R. Hoffman, Inorg. Chem. **24**, 4108 (1985); M. Drillon, M. Belaiche, P. Legoll, J. Aride, A. Boukhari, and A. Moquine, J. Magn. Magn. Mater. **128**, 83 (1993); A. Shengelaya, G. I. Meijer, J. Karpinski, Guo-meng Zhao, H. Schwer, E. M. Kopnin, C. Rossel, and H. Keller, Phys. Rev. Lett. **80**, 3626 (1998); P. Horsch, M. Sofin, M. Mayr, and M. Jansen, *ibid.* **94**, 076403 (2005); H. Kikuchi, Y. Fujii, M. Chiba, S. Mitsudo, T. Idehara, T. Tonegawa, K. Okamoto, T. Sakai, T. Kuwai, and H. Ohta, *ibid.* **94**, 227201 (2005).

[19] G. Obermair, in *Dynamical Aspects of Critical Phenomena*, edited by J. I. Budnick and M. P. Kawatra (Gordon and Breach, New York, 1972), p. 137.

[20] A. M. S. Mâcedo, M. C. dos Santos, M. D. Coutinho-Filho, and C. A. Mâcedo, Phys. Rev. Lett. **74**, 1851 (1995); G. S. Tian and T. H. Lin, Phys. Rev. B **53**, 8196 (1996); G. Sierra, M. A. Mártin-Delgado, S. P. White, D. J. Scalapino, and J. Dukelsky, *ibid.* **59**, 7973 (1999); R. R. Montenegro-Filho and M. D. Coutinho-Filho, Physica A **357**, 173 (2005).

[21] F. C. Alcaraz and A. L. Malvezzi, J. Phys. A **30**, 767 (1997); E. P. Raposo and M. D. Coutinho-Filho, Phys. Rev. Lett. **78**, 4853 (1997); Phys. Rev. B **59**, 14384 (1999); T. Nakanishi and S. Yamamoto, *ibid.* **65**, 214418 (2002).

[22] C. Vitoriano, M. D. Coutinho-Filho, and E. P. Raposo, J. Phys. A **35**, 9049 (2002); C. Vitoriano, F. B. de Brito, E. P. Raposo, and M. D. Coutinho-Filho, Mol. Cryst. Liq. Cryst. Sci. Technol., Sect. A **374**, 185 (2002).

[23] The AF coupling is chosen so as to relate the quantum spherical AB_2 model to the strong-coupling half-filled AB_2 Hubbard model and its associated quantum AF AB_2 Heisenberg model: E. P. Raposo and M. D. Coutinho-Filho, Mod. Phys. Lett. B **9**, 817 (1995).

[24] S. Sachdev and T. Senthil, Ann. Phys. (N.Y.) **251**, 76 (1996).

[25] E. H. Lieb, Phys. Rev. Lett. **62**, 1201 (1989).

[26] See, e.g., R. K. Pathria, *Statistical Mechanics* (Elsevier, Oxford, 2004), p. 389, and references therein.

[27] M. E. Fisher, Am. J. Phys. **32**, 343 (1964).

[28] M. Takahashi and M. Yamada, J. Phys. Soc. Jpn. **54**, 2808 (1985); M. Takahashi, Phys. Rev. Lett. **58**, 168 (1987).

[29] J. L. Lebowitz and J. K. Percus, Phys. Rev. **144**, 251 (1966); G. S. Joyce, *ibid.* **146**, 349 (1966); G. Stell, *ibid.* **184**, 135 (1969).